J. Biochem. **140**, 121–133 (2006)
doi:10.1093/jb/mvj136

Mutational and Functional Analysis of the Cryptic N-Terminal Targeting Signal for Both Mitochondria and Peroxisomes in Yeast Peroxisomal Citrate Synthase Cit2p

Jeong Goo Lee[1,*], Yong Joo Lee[1], Cheong Ho Lee[2] and Pil Jae Maeng[1,†]
[1]Department of Microbiology, School of Biological Science & Biotechnology, Chungnam National University, Daejeon 305-764; and [2]KT&G Central Research Institute, Daejeon 305-805, Korea

Received April 23, 2006; accepted May 22, 2006

We previously found that the peroxisomal citrate synthase of *Saccharomyces cerevisiae*, Cit2p, contains a cryptic targeting signal for both peroxisomes (PTS) and mitochondria (MTS) within its 20–amino acid N-terminal segment [Lee *et al.* (2000) *J. Biochem.* 128, 1059–1072]. In the present study, the fine structure of the cryptic signal was scrutinized using green fluorescent protein fusions led by variants of the N-terminal segment. The minimum ranges of the cryptic signals for mitochondrial and peroxisomal targeting were shown to consist of the first 15– and 10–amino acid N-terminal segments, respectively. Substitution of the 3rd Val, 6th Leu, 7th Asn, or 8th Ser with Ala abolished the cryptic MTS function, however, no single substitution causing an obvious defect in PTS function was found. Neither the 15–amino acid N-terminal segment nor the C-terminal SKL sequence (PTS1) was necessary for Cit2p to restore the glutamate auxotrophy caused by the double Δ*cit1* Δ*cit2* mutation. The Cit2p variant lacking PTS1 [Cit2(ΔSKL)p] partially restored the growth of both the Δ*cit1* Δ*cit2* and Δ*cit1* mutants on acetate, while that carrying intact PTS1 or lacking the N-terminal segment [Cit2p, Cit2$_{(\Delta N \Delta SKL)}$p, and Cit2$_{(\Delta N)}$p] did not. It is thus suggested that the potential of the N-terminal segment as an ambidextrous targeting signal can be unmasked by deletion of PTS1.

Key words: citrate synthase (Cit2p), cryptic targeting signal, green fluorescent protein, mitochondria, N-terminal segment, peroxisomes.

Abbreviations: GFP, green fluorescent protein; PTS1, peroxisomal targeting signal 1; PTS2, peroxisomal targeting signal 2; MTS, mitochondrial targeting signal; *CIT1*, gene encoding mitochondrial citrate synthase; *CIT2*, gene encoding peroxisomal citrate synthase; *PEX5*, gene encoding PTS1 receptor; *PEX7*, gene encoding PTS2 receptor.

In eukaryotic cells, two different organelles often share a variety of common metabolic reactions. In some cases, one common reaction is catalyzed by a single enzyme which is encoded by a single corresponding gene and imported into the two different organelles. For example, both the nuclear and mitochondrial forms of uracil-DNA glycosylase of man are encoded by *UNG15* cDNA, and the signals for mitochondrial and nuclear translocation reside in the presequence of the precursor form and the internal segment of the mature protein, respectively (*1*). In the case of mitochondrial (SPTm) and peroxisomal serine:pyruvate aminotransferases (SPTp) of rat river, the 5′-terminal sequence of SPTm mRNA is about 70 nucleotides longer than that of SPTp mRNA, which indicates that the different organellar distribution of SPTm and SPTp arises from transcription from different initiation sites, conferring the N-terminal extension peptide, the mitochondrial targeting signal, only on the translation product of SPTm mRNA (*2*). In the filamentous fungus *Aspergillus nidulans*, two different transcripts are formed from a single *idpA* gene encoding NADP-dependent isocitrate dehydrogenase by using two transcription start points. While the longer transcript encodes a polypeptide containing an N-terminal mitochondrial targeting sequence (MTS) as well as a C-terminal tripeptide (ARL) as a potential peroxisomal targeting signal (PTS1), the shorter one encodes a polypeptide lacking the MTS but retaining the PTS1. Therefore, through the use of two transcription start points a single gene is sufficient to specify the localization of NADP-dependent isocitrate dehydrogenase to two different organelles (*3*).

More frequently, each of the common reactions is catalyzed by two or more isofunctional enzymes that are encoded by different genes and imported into their own destined organelles by means of specific signal sequences. For example, *Saccharomyces cerevisiae* has three distinct citrate synthases [EC 4.1.3.7] that catalyze the formation of citrate from acetyl-CoA and oxaloacetate, and are encoded by three different genes, *CIT1* (*4*), *CIT2* (*5*), and *CIT3* (*6*). The major mitochondrial citrate synthase, Cit1p, is transported into the mitochondrial matrix, where it functions as the rate-limiting enzyme of the TCA cycle by means of an N-terminal MTS (*4*). On the other hand, the peroxisomal citrate synthase, Cit2p, has a PTS1 (SKL tripeptide sequence) at its C-terminus and is targeted to peroxisomes, where it is involved in the glyoxylate cycle (*7*).

We have found that the 37–amino acid N-terminal segment of Cit1p is removed in the process of mitochondrial

[†]To whom correspondence should be addressed. Tel: +82-42-821-6415, Fax: +82-42-821-6415, E-mail: pjmaeng@cnu.ac.kr
*Present address: Doheny Eye Institute, Univ. Southern California, 1450 San Pablo St. DVRC 203, Los Angeles, CA 90033, USA.

targeting through proteolytic cleavage at the R-3 motif [$R_{(35)}$-H-Y ↓ $S_{(38)}$] and that, although Cit2p has a C-terminal PTS1, its N-terminal segment is removed during import into peroxisomes (*8*, *9*). We have also shown that the 20–amino acid N-terminal segment of Cit2p contains a cryptic cleavable targeting signal for both peroxisomes and mitochondria, and further that the peroxisomal import process mediated by the N-terminal segment of Cit2p is not affected by disruption of either *PEX5* (encoding PTS1 receptor) or *PEX7* (encoding PTS2 receptor) (*10*).

In the present study, to scrutinize the fine structure and function of the cryptic N-terminal signal of Cit2p, we analyzed the behavior of fusion proteins containing various mutant versions of the N-terminal segment Cit2p and green fluorescent protein (GFP2). We also examined the physiological role of the cryptic signal by analyzing the growth characteristics of the transformants (Δ*cit1* Δ*cit2*) expressing various mutant versions of Cit1p or Cit2p. The results of these studies are presented.

MATERIALS AND METHODS

Strains, Media and Transformation—*S. cerevisiae* strains were grown on either YPD (complete medium), YPA (same as YPD, except that 2% of glucose was replaced by 2% of sodium acetate), or YNB (minimal medium containing 2% of glucose as a sole carbon source and supplemented with 0.68 mM of lysine) (*8*). Transformation of *S. cerevisiae* strains was performed by using the lithium acetate method (*11*). The *S. cerevisiae* strains used in this study are listed in Table 1. To examine the cultural characteristics of *S. cerevisiae* strains on solid media, cells grown overnight in liquid YPD were washed and suspended in phosphate-buffered saline (PBS, pH 7.4) to the concentration of 1.0×10^8 cells ml^{-1}. After the cell suspensions had been serially diluted in 10-fold steps, a 3 μl aliquot of each dilution was applied on appropriate solid minimal media and the plates were incubated at 30°C or other desired temperatures. For growth assays in liquid media, aliquots of the cell suspension were inoculated into proper liquid media at the concentration of 1.0×10^4 cells ml^{-1} and the cells were grown with shaking at 30°C.

E. coli DH5α cells were grown in Luria-Bertani (LB) medium and transformed with the use of standard methods (*12*).

Construction of Plasmids—The plasmids used in this study are also listed in Table 1. Hybrid genes encoding the fusion proteins which contained the N-terminal segment of Cit2p with varying numbers (from 9 to 19) of amino acid residues and GFP2 were constructed individually as follows. First, the 0.75-kb *Kpn*I–*Eco*RI *gfp2* cDNA in which the initiation codon is substituted by a coding sequence for five or six additional amino acid residues, (L/V)VPVEK, was amplified from pGFP2 (*10*) by PCR using a pair of primers, P1 (5′-GGTACCGGTAGAAAAAAGTAAAGGAGAAGAACTT-3′) and P2 (5′-GAATTCCTATTTGTATAGTTCATCCAT-3′), and then cloned into the *Eco*RV site of the pT7Blue(R) plasmid (Novagen) to yield pT7GFP2. PCR was performed with a DNA thermal cycler (GeneAmp PCR system 2400; Perkin-Elmer Cetus) using *Taq* DNA polymerase (Boehringer Mannheim). YEplacGFP2 was constructed by cloning the 0.75-kb *Kpn*I–*Eco*RI *gfp2* fragment from pT7GFP2 into *Kpn*I–*Eco*RI–digested YEplac181. In parallel, each of the *cit2* fragments containing the promoter region (*cit2-p*) and the coding sequences for the N-terminal segments of Cit2p of variable length was amplified individually from YEpCit2$_{(1–65)}$::GFP2 (*10*) by using a pair of primers, RP (reverse primer, 5′-AACAGCTAGACCATG-3′) and one of the following: P9d (5′GGTACGGTACCAAGTTTGAATTTAGATAAGG3′), P10d (5′GGTACCCTGTTTGAATTTAGATAAGG3′), P11d (5′GGTACCAAATTTCTGTTTGAATTTAG3′), P12d (5′GGTACCACATTTCTGTTTGAATTTAG3′), P13d (5′GGTACCGCAACATTTCTGTTTGAATTT3′), P14d (5′GGTACCACTGATGCAACATTTCTGTTTG3′), P15d (5′GGTACCACATATGATGCAACATTTCTGT3′), P16d (5′GGTACCACTAAATATGATGCAACATTTC3′), P17d (5′GGTACCACTTGTAAATATGATGCAAC3′), P18d (5′GGTACCACTGATTGTAAATATGATG3′), and P19d (5′GGTACCACATTTGATTGTAAATATGA3′). Each of the PCR-amplified *cit2* fragments was cloned into the *Eco*RV site of the pT7 Blue(R) plasmid, excised from the vector by *Hin*dIII–*Kpn*I double digestion, and then inserted individually into *Hin*dIII–*Kpn*I–digested YEplacGFP2 to yield the following recombinants: YEpCit2$_{(1–9)}$::GFP2, YEpCit2$_{(1–10)}$::GFP2, YEpCit2$_{(1–11)}$::GFP2, YEpCit2$_{(1–12)}$::GFP2, YEpCit2$_{(1–13)}$::GFP2, YEpCit2$_{(1–14)}$::GFP2, YEpCit2$_{(1–15)}$::GFP2, YEpCit2$_{(1–16)}$::GFP2, YEpCit2$_{(1–17)}$::GFP2, YEpCit2$_{(1–18)}$::GFP2, and YEpCit2$_{(1–19)}$::GFP2 (Fig. 1A).

Hybrid genes encoding the fusion proteins which contained the 20–amino acid N-terminal segments of Cit2p with single amino acid substitutions at positions from 15 to 20 and GFP2 were constructed individually as follows. First, each of the *cit2* fragments containing the promoter region (*cit2-p*) and one of the coding sequences for the N-terminal segments of Cit2p with the single substitutions was amplified individually from YEpCit2$_{(1–20)}$::GFP2 by using a pair of primers, RP and one of the following (italic characters denote the modified codons for site-directed mutagenesis, and N and R any base and either purine, respectively): PY15X (5′GGTACCACATTTGATTACATTTGATTGTAA*RNN*TGA3′), PL16X (5′GGTACCACACATTTGATTG*RNN*ATATGA3′), PQ17X (5′GGTACCACATTTGA*RNN*TAAATATGA3′), PS18X (5′GGTACCACATT*RNN*TTGTAAATATGA3′), PN19X (5′GGTACCAC*RNN*TGATTGTAAATATGA3′), and PS20X (5′GGTAC*CNN*ATTTGATTGTAAATATGA3′). Then each of the PCR-amplified *cit2* fragments was cloned into the *Eco*RV site of the pT7Blue(R) plasmid, excised from the vector by *Hin*dIII–*Kpn*I double digestion, and then inserted individually into *Hin*dIII–*Kpn*I–digested YEplacGFP2 to yield the following recombinants: YEpCit2$_{(Y15F)}$::GFP2, YEpCit2$_{(Y15P)}$::GFP2, YEpCit2$_{(Y15S)}$::GFP2, YEpCit2$_{(L16A)}$::GFP2, YEpCit2$_{(Q17P)}$::GFP2, YEpCit2$_{(Q17R)}$::GFP2, YEpCit2$_{(S18P)}$::GFP2, YEpCit2$_{(N19A)}$::GFP2, YEpCit2$_{(N19F)}$::GFP2, YEpCit2$_{(N19L)}$::GFP2, YEpCit2$_{(N19P)}$::GFP2, YEpCit2$_{(N19S)}$::GFP2, and YEpCit2$_{(S20L)}$::GFP2 (Fig. 1A).

Hybrid genes encoding the fusion proteins which contained the 15–amino acid N-terminal segment of Cit2p with single amino acid substitutions (X→Ala at positions from 2 to 15 except for 13) and GFP2 were constructed similarly. First, each of the *cit2* fragments containing the coding sequence for one of the N-terminal segments of Cit2p with the single substitutions led by the promoter region (*cit2-p*) was amplified individually from

Table 1. *S. cerevisiae* strains and plasmids used in this study.

Strain and plasmid	Relevant genotype	Reference or source
PSY37	*leu2–3 leu2–112 ura3–52 lys2–801*	(*9*)
PSY38	*cit1::LEU2 leu2–3 leu2–112 ura3–52 lys2–801*	(*8*)
PSY40	*cit2::URA3 leu2–3 leu2–112 ura3–52 lys2–801*	(*8*)
MPY001	*cit1::LEU2 cit2::ura3–508 leu2–3 leu2–112 ura3–52 lys2–801*	(*10*)
pPLCS1	*CIT1 LEU2*	(*8*)
pUCS2	*CIT2 URA3*	(*8*)
YEpCit1	*CIT1 URA3*	This study
YEpCit1$_{(\Delta N)}$	*cit1-ΔN URA3*	This study
YEpCit1$_{(SKL)}$	*cit1-SKL URA3*	This study
YEpCit1$_{(\Delta N\text{-}SKL)}$	*cit1-ΔN-SKL URA3*	This study
YEpCit2	*CIT2 URA3*	This study
YEpCit2$_{(\Delta N)}$	*cit2-ΔN URA3*	This study
YEpCit2$_{(\Delta SKL)}$	*cit2-ΔSKL URA3*	This study
YEpCit2$_{(\Delta N\Delta SKL)}$	*cit2-ΔNΔSKL URA3*	This study
YEpCit1$_{(1–38)}$::GFP2	*cit1–38::gfp2 URA3*	(*10*)
YEpCit2$_{(p)}$::GFP2	*cit2-p::gfp2 LEU2*	(*10*)
YEpCit2$_{(p)}$::GFP2-SKL	*cit2-p::gfp2-SKL LEU2*	(*10*)
YEpCit2$_{(1–9)}$::GFP2	*cit2–9::gfp2 LEU2*	This study
YEpCit2$_{(1–10)}$::GFP2	*cit2–10::gfp2 LEU2*	This study
YEpCit2$_{(1–11)}$::GFP2	*cit2–11::gfp2 LEU2*	This study
YEpCit2$_{(1–12)}$::GFP2	*cit2–12::gfp2 LEU2*	This study
YEpCit2$_{(1–13)}$::GFP2	*cit2–13::gfp2 LEU2*	This study
YEpCit2$_{(1–14)}$::GFP2	*cit2–14::gfp2 LEU2*	This study
YEpCit2$_{(1–15)}$::GFP2	*cit2–15::gfp2 LEU2*	This study
YEpCit2$_{(1–16)}$::GFP2	*cit2–16::gfp2 LEU2*	This study
YEpCit2$_{(1–17)}$::GFP2	*cit2–17::gfp2 LEU2*	This study
YEpCit2$_{(1–18)}$::GFP2	*cit2–18::gfp2 LEU2*	This study
YEpCit2$_{(1–19)}$::GFP2	*cit2–19::gfp2 LEU2*	This study
YEpCit2$_{(1–20)}$::GFP2	*cit2–20::gfp2 LEU2*	(*10*)
YEpCit2$_{(T2A)}$::GFP2	*cit2–15(T2A)::gfp2 LEU2*	This study
YEpCit2$_{(V3A)}$::GFP2	*cit2–15(V3A)::gfp2 LEU2*	This study
YEpCit2$_{(P4A)}$::GFP2	*cit2–15(P4A)::gfp2 LEU2*	This study
YEpCit2$_{(Y5A)}$::GFP2	*cit2–15(Y5A)::gfp2 LEU2*	This study
YEpCit2$_{(L6A)}$::GFP2	*cit2–15(L6A)::gfp2 LEU2*	This study
YEpCit2$_{(N7A)}$::GFP2	*cit2–15(N7A)::gfp2 LEU2*	This study
YEpCit2$_{(S8A)}$::GFP2	*cit2–15(S8A)::gfp2 LEU2*	This study
YEpCit2$_{(N9A)}$::GFP2	*cit2–15(N9A)::gfp2 LEU2*	This study
YEpCit2$_{(R10A)}$::GFP2	*cit2–15(R10A)::gfp2 LEU2*	This study
YEpCit2$_{(N11A)}$::GFP2	*cit2–15(N11A)::gfp2 LEU2*	This study
YEpCit2$_{(V12A)}$::GFP2	*cit2–15(V12A)::gfp2 LEU2*	This study
YEpCit2$_{(S14A)}$::GFP2	*cit2–15(S14A)::gfp2 LEU2*	This study
YEpCit2$_{(Y15A)}$::GFP2	*cit2–15(Y15A)::gfp2 LEU2*	This study
YEpCit2$_{(Y15F)}$::GFP2	*cit2–20(Y15F)::gfp2 LEU2*	This study
YEpCit2$_{(Y15P)}$::GFP2	*cit2–20 (Y15P)::gfp2 LEU2*	This study
YEpCit2$_{(Y15S)}$::GFP2	*cit2–20 (Y15S)::gfp2 LEU2*	This study
YEpCit2$_{(L16A)}$::GFP2	*cit2–20 (L16A)::gfp2 LEU2*	This study
YEpCit2$_{(Q17P)}$::GFP2	*cit2–20 (Q17P)::gfp2 LEU2*	This study
YEpCit2$_{(Q17R)}$::GFP2	*cit2–20 (Q17R)::gfp2 LEU2*	This study
YEpCit2$_{(S18P)}$::GFP2	*cit2–20(S18P)::gfp2 LEU2*	This study
YEpCit2$_{(N19A)}$::GFP2	*cit2–20(N19A)::gfp2 LEU2*	This study
YEpCit2$_{(N19F)}$::GFP2	*cit2–20(N19F)::gfp2 LEU2*	This study
YEpCit2$_{(N19P)}$::GFP2	*cit2–20(N19P)::gfp2 LEU2*	This study
YEpCit2$_{(N19S)}$::GFP2	*cit2–20(N19S)::gfp2 LEU2*	This study
YEpCit2$_{(S20L)}$::GFP2	*cit2–20(S20L)::gfp2 LEU2*	This study

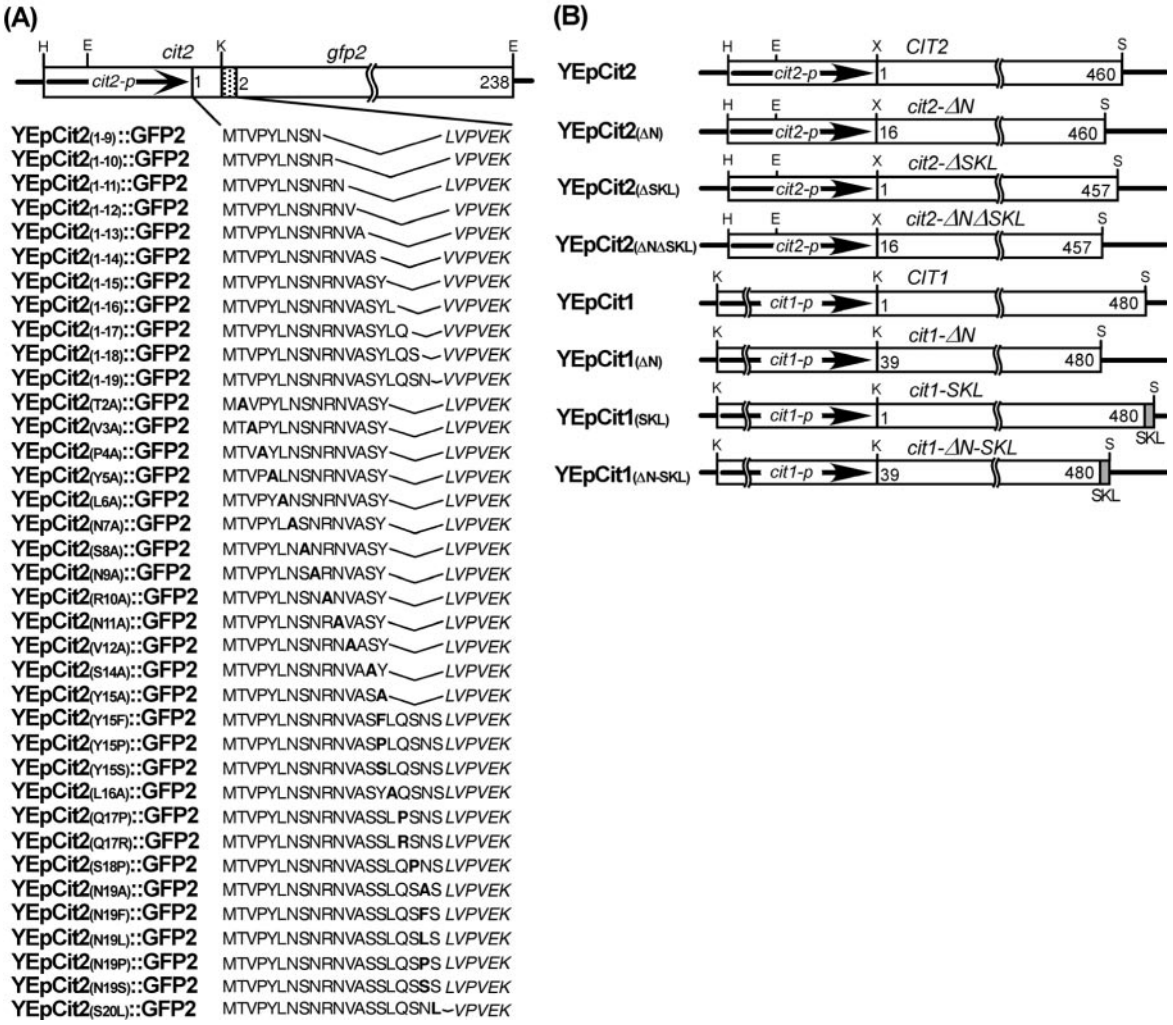

Fig. 1. **Construction of chimeric genes encoding Cit2p::GFP2 fusion proteins and mutant alleles of *CIT1* or *CIT2*.** (A) Structures of the chimeric genes encoding various Cit2p::GFP2 fusions. The promoter region of *CIT2* (*cit2-p*) is indicated by a solid arrow. Numerals in each bar refer to the amino acid positions at the boundaries of the polypeptide segment encoded by the allele. The amino acid sequences of the N-terminal segments of the fusion proteins are presented with one-letter abbreviations. The italicized amino acid sequences denote the additional junctions between the N-terminal segments of Cit2p and GFP2, and the boldfaced characters denote the substitution of the original amino acid residues. (B) Structures of *CIT1*, *CIT2*, and their mutant alleles. The promoter regions of *CIT1* (*cit1-p*) and *CIT2* (*cit2-p*) are indicated by solid arrows. Numerals in each bar refer to the amino acid positions at the boundaries of the polypeptide segment encoded by the allele. Restriction enzyme sites: E, *Eco*RI; H, *Hin*dIII; K, *Kpn*I; S, *Sac*I; X, *Xba*I.

YEpCit2$_{(1–15)}$::GFP2 by using a pair of primers, RP and one of the following (italic characters denote the modified codons for site-directed mutagenesis): PT2A (5′GGTACCAAATATGATGCAACATTTCTGTTTGAATTTAGATAAGGAAC*TGC*CATTTT3′), PV3A (5′GGTACCAAATATGATGCAACATTTCTGTTTGAATTTAGATAAGG*AGC*TGTCAT3′), PP4A (5′GGTACCAAATATGATGCAACATTTCTGTTTGAATTTAGATA*AGC*AACTGT3′), PY5A (5′GGTACCAAATATGATGCAACATTTCTGTTTGAATTTAG*AGC*AGGAAC3′), PL6A (5′GGTACCAAATATGATGCAACATTTCTGTTTGAATT*TGC*ATAAGG3′), PN7A (5′GGTACCAAATATGATGCAACATTTCTGTTTGA*AGC*TAGATA3′), PS8A (5′GGTACCAAATATGATGCAACATTTCTGTTT*TGC*ATTTAG3′), PN9A (5′GGTACCAAATATGATGCAACATTTCTA*GC*TGAATT3′), PR10A (5′GGTACCAAATATGATGCAACATT*TGC*GTTTGA3′), PN11A (5′GGTACCAAATATGATGCAAC*AGC*TCTGTT3′), PV12A (5′GGTACCAAATATGATGC*AGC*ATTTCTG3′), PS14A (5′GGTACCAAATA*TGC*TGCAACATTTCTG3′), and PY15A (5′GGTACCAA*AGC*TGATGCAACATTTCTG3′). Then each of the PCR-amplified *cit2* fragments was cloned into the *Eco*RV site of the pT7Blue(R) plasmid, excised from the vector by *Hin*dIII–*Kpn*I double digestion, and then inserted individually into *Hin*dIII–*Kpn*I–digested YEplacGFP2 to yield the following recombinants: YEpCit2$_{(T2A)}$::GFP2, YEpCit2$_{(V3A)}$::GFP2, YEpCit2$_{(P4A)}$::GFP2, YEpCit2$_{(Y5A)}$::GFP2, YEpCit2$_{(L6A)}$::GFP2, YEpCit2$_{(N7A)}$::GFP2, YEpCit2(S8A)::GFP2, YEpCit2$_{(N9A)}$::GFP2, YEpCit2$_{(R10A)}$::GFP2, YEpCit2$_{(N11A)}$::GFP2, YEpCit2$_{(V12A)}$::GFP2, YEpCit2$_{(S14A)}$::GFP2, and YEpCit2$_{(Y15A)}$::GFP2 (Fig. 1A).

Plasmids carrying *CIT2* or one of its mutant alleles, *cit2-ΔN*, *cit2-ΔSKL*, and *cit2-ΔNΔSKL*, were constructed as follows. First, the promoter region of *CIT2* (*cit2-p*) was

amplified from YEpCit2$_{(1–9)}$::GFP2 by using a pair of primers, RP and P3 (5′-TCTAGATTTTCTTGTTACTAGTATTA-3′), and then cloned into pT7Blue(R) to yield pT7Cit2$_{(p)}$. The 0.35-kb *Hin*dIII–*Xba*I *cit2-p* fragment was excised from pT7Cit2$_{(p)}$ and inserted into *Hin*dIII–*Xba*I–digested YEp352 to yield YEp352Cit2$_{(p)}$. In parallel, four different *cit2* fragments encoding the full-length or deleted versions of Cit2p were amplified individually from pUCS2 by using four different combinations of primers: *cit2–460* (coding sequence for full-length Cit2p) by using P4 (5′-TCTAGAATGACAGTTCCTTATCTAAAT-3′) and P6 (5′-GAGCTCCTATAGTTTGCTTTCAATGTT-3′), *cit2–445* (coding sequence for Cit2p variant lacking the 15–amino acid N-terminal segment) by using P5 (5′-TCTAGAATGTTACAATCAAATTCAAGCCAA-3′) and P6, *cit2–457* (coding sequence for Cit2p variant lacking the C-terminal SKL sequence) by using P4 and P7 (5′-GAGCTCCTATTCAATGTTTTTGACCAATTC-3′), and *cit2–442* (coding sequence for Cit2p variant lacking both the 15–amino acid N-terminal segment and the C-terminal SKL sequence) by using P5 and P7. Then the PCR-amplified *cit2* segments, *cit2–460*, *cit2–445*, *cit2–457*, and *cit2–442*, were cloned into pT7Blue(R) to yield pT7Cit2$_{(460)}$, pT7Cit2$_{(445)}$, pT7Cit2$_{(457)}$, and pT7Cit2$_{(442)}$, respectively. Finally, each of the four *cit2* segments was excised by *Xba*I–*Sac*I double digestion and inserted into *Xba*I–*Sac*I–digested YEp352Cit2$_{(p)}$ downstream of the *cit2-p* to yield YEpCit2, YEpCit2$_{(ΔN)}$, YEpCit2$_{(ΔSKL)}$, and YEpCit2$_{(ΔNΔSKL)}$ carrying the *CIT2*, *cit2-ΔN*, *cit2-ΔSKL*, and *cit2-ΔNΔSKL* alleles, respectively (Fig. 1B).

Four recombinant plasmids carrying *CIT1* or one of the mutant alleles, *cit1-ΔN*, *cit1-SKL*, or *cit1-ΔN-SKL*, were constructed as follows. First, four different *cit1* fragments encoding the full-length or deleted variants of Cit1p were amplified individually from chromosomal DNA by using four different combinations of primers: *cit1–480* (coding sequence for full-length Cit1p) by using P8 (5′-GGTACCATGTCAGCGATATTA-3′) and P9 (5′-GAGCTCTTAGTTCTTACTTTC-3′), *cit1–442* (coding sequence for Cit1p variant lacking the 38–amino acid N-terminal segment, MTS) by using P10 (5′-GGTACCATGAGCGCCTCCGAACAA-3′) and P9, *cit1–483* (coding sequence for Cit1p variant containing an additional C-terminal SKL sequence) by using P8 and P11 (5′-GAGCTCTTATAGTTTGCTGTTCTTACTTTCGATTTT-3′), and *cit1–445* (coding sequence for Cit1p variant lacking the 38–amino acid N-terminal segment but containing an additional C-terminal SKL sequence) by using P10 and P11 primers. The PCR-amplified *cit1* segments, *cit1–480*, *cit1–442*, *cit1–483*, and *cit1–445*, were cloned into pT7Blue(R) to yield pT7Cit1$_{(480)}$, pT7Cit1$_{(442)}$, pT7Cit1$_{(483)}$, and pT7Cit1$_{(445)}$, respectively. Each of the four *cit1* segments was then excised by *Kpn*I–*Sac*I double digestion and inserted into *Kpn*I–*Sac*I–digested YEp352 to yield YEp352Cit1$_{(480)}$, YEp352Cit1$_{(442)}$, YEp352Cit1$_{(483)}$, and YEp352Cit1$_{(445)}$, respectively. In parallel, the promoter region of *CIT1* (*cit1-p*) was amplified from chromosomal DNA by using a pair of primers, P12 (5′-GAATTCCGCAATTTTCCAACCATTAG-3′) and P13 (5′-GGTACCCTTCGTAAATAGTATTATAT-3′), and cloned into pT7Blue(R) to yield pT7Cit1$_{(p)}$. The 0.63-kb *Kpn*I *cit1-p* fragment was excised from pT7Cit1$_{(p)}$ and inserted into *Kpn*I-digested YEp352Cit1$_{(480)}$, YEp352Cit1$_{(442)}$, YEp352Cit1$_{(483)}$, and YEp352Cit1$_{(445)}$, to yield YEpCit1, YEpCit1$_{(ΔN)}$, YEpCit1$_{(SKL)}$, and YEpCit1$_{(ΔN-SKL)}$, respectively (Fig. 1B).

Cell Fractionation—For cell fractionation, one gram (wet weight) of washed yeast cells was suspended in 7 ml of 0.1 M Tris-SO$_4$ buffer (pH 8.5) containing 10 mM dithiothreitol and then incubated at 30°C for 30 min. After a rinse with 1.2 M sorbitol, the cells were resuspended in isotonic buffer (1.2 M sorbitol in 20 mM potassium phosphate, pH 7.4) and treated with lyticase [1,000 to 2,500 units (g cell wet weight)$^{-1}$; Sigma] at 30°C for 1.5 h. The resulting spheroplasts were harvested by centrifugation (3,000 × *g*), resuspended in lysis buffer (0.6 M sorbitol, 1 mM KCl and 0.5 mM EDTA in 5 mM MES-KOH buffer, pH 6.0), and then homogenized in a Dounce glass homogenizer. The cell debris was removed by centrifugation (1,500 × *g*, 10 min), and the organelles were harvested (25,00 × *g*, 20 min). The organelles were resuspended in 5 mM MES-KOH buffer (pH 6.0) containing 0.24 M sucrose and 1 mM EDTA, and then fractionated by ultracentrifugation through a step gradient prepared with 17, 25 and 35% Nycodenz solutions in the same buffer. Ultracentrifugation (Beckman LE-80) was carried out in a SW55Ti rotor at 112,000 × *g* for 90 min at 4°C. Each fraction from the gradient was diluted 5-fold with 5 mM MES-KOH buffer (pH 6.0) containing 0.24 M sucrose and 1 mM EDTA, and the Nycodenz was removed by centrifugation at 25,000 × *g* for 20 min. For immunoblotting and enzyme assaying, the organelles were ruptured by adding Triton X-100 up to 1%.

Immunoblotting—Immunoblotting was carried out by the enhanced chemiluminescence method (ECL; Amersham). The primary antibodies were the mouse monoclonal anti-Cox3p (cytochrome c oxidase subunit III of *S. cerevisiae*; Molecular Probes), rabbit anti-GFP (Clontech), mouse anti-Eno1p (enolase; donated by Dr. Hee-Moon Park, Chungnam National University), rabbit anti-Cta1p (*10*), and rabbit anti-Cit1p antibodies (*10*). The secondary antibodies were horseradish peroxidase–conjugated anti-rabbit IgG and anti-mouse IgG (Kirkegaard and Perry).

Citrate Synthase Assay—Citrate synthase was assayed by the 5,5′-dithiobis-(2-nitrobenzoic acid) (DTNB) method (*13*).

RESULTS

Determination of the Minimum Extent of the N-Terminal Targeting Signal of Cit2p—We found in the previous research that the cryptic ambidextrous targeting signal located in the N-terminal region of Cit2p requires more than 8 but not more than 20 N-terminal amino acids to be able to guide the cargo protein (GFP2) either to mitochondria or peroxisomes (*10*). In the present study, we constructed chimeric genes which encode the GFP2 fusion proteins carrying anteriorly fused N-terminal segments of Cit2p with varying numbers (from 9 to19) of amino acids to define the minimum extent of the targeting signal. The hybrid genes contained in the high-copy plasmids were individually introduced into the wild-type strain (PSY37; *CIT1 CIT2*) of *S. cerevisiae*. The resulting transformants were analyzed for the subcellular localization of the fusion proteins by fractionation of intracellular organelles followed by immunoblotting in comparison with those previously reported, such as the YEpCit2$_{(p)}$::GFP2,

YEpCit1$_{(1–38)}$::GFP2, and YEpCit2$_{(p)}$::GFP2-SKL transformants expressing GFP2, Cit1$_{(1–38)}$::GFP2, and GFP2-SKL, respectively (*10*).

It was confirmed in the previous study that Cit1$_{(1–38)}$::GFP2 carrying the N-terminal cleavable MTS of Cit1p and GFP2-SKL carrying a C-terminal PTS1 are targeted to mitochondria and peroxisomes, respectively, while GFP2 itself is not imported into any organelles and thus remains in the cytosol. As shown in Fig. 2, each of the transformants producing the Cit2$_{(1–19)}$::GFP2, Cit2$_{(1–18)}$::GFP2, Cit2$_{(1–17)}$::GFP2, Cit2$_{(1–16)}$::GFP2, and Cit2$_{(1–15)}$::GFP2 fusion proteins, respectively, gave a 27-kDa single band binding to anti-GFP antibodies for both the mitochondrial and peroxisomal fractions as well as the cytosolic fraction. On the other hand, the transformants expressing the Cit2$_{(1–14)}$::GFP2, Cit2$_{(1–13)}$::GFP2, Cit2$_{(1–12)}$::GFP2, Cit2$_{(1–11)}$::GFP2, and Cit2$_{(1–10)}$::GFP2 fusion proteins, respectively, gave a single positive band for the peroxisomal and cytosolic fractions but not for the mitochondrial fraction at all. The transformant producing Cit2$_{(1–9)}$::GFP2, however, did not show any positive signals for either of the organelle fractions, and showed one only for the cytosolic fraction.

This result suggests that the minimum extent for functioning of the cryptic signal for mitochondrial targeting of cargo proteins consists of the N-terminal 15–amino acid residues of Cit2p (Fig. 4A). As a matter of course, it turns out that the 15–amino acid N-terminal segment is the minimum requirement for the cryptic dual targeting signal of Cit2p. In addition, it was also revealed that the minimum requirement for peroxisomal targeting of cargo proteins to peroxisomes is the 10–amino acid N-terminal segment of Cit2p (Fig. 4A).

Determination of the Amino Acid Residues Essential for the Cryptic N-Terminal Targeting Signal of Cit2p—To define the amino acids essential for the cryptic N-terminal signal of Cit2p for mitochondrial and/or peroxisomal targeting, hybrid genes encoding GFP2 fusion proteins carrying anteriorly fused 20– or 15–amino acid N-terminal segments of Cit2p with single amino acid substitutions were constructed and individually introduced into *S. cerevisiae* PSY37. Then the subcellular localization of the fusion proteins expressed in each transformant was analyzed by fractionation of intracellular organelles followed by immunoblotting.

Each of the transformants expressing Cit2$_{(L16A)}$::GFP2, Cit2$_{(Q17P)}$::GFP2, Cit2$_{(Q17R)}$::GFP2, Cit2$_{(S18P)}$::GFP2, Cit2$_{(N19A)}$::GFP2, Cit2$_{(N19F)}$::GFP2, Cit2$_{(N19L)}$::GFP2, Cit2$_{(N19P)}$::GFP2, Cit2$_{(N19S)}$::GFP2, and Cit2$_{(S20L)}$::GFP2 fusion proteins, respectively, gave a single band of approx. 27 kDa recognized by anti-GFP antibodies for the mitochondrial, peroxisomal, and cytosolic fractions (data not shown). This result suggests that no single substitution of the amino acids located at positions 16 to 20 affects the function of the 15–amino acid cryptic N-terminal targeting signal at all (Fig. 4A). Together with the results of serial deletion

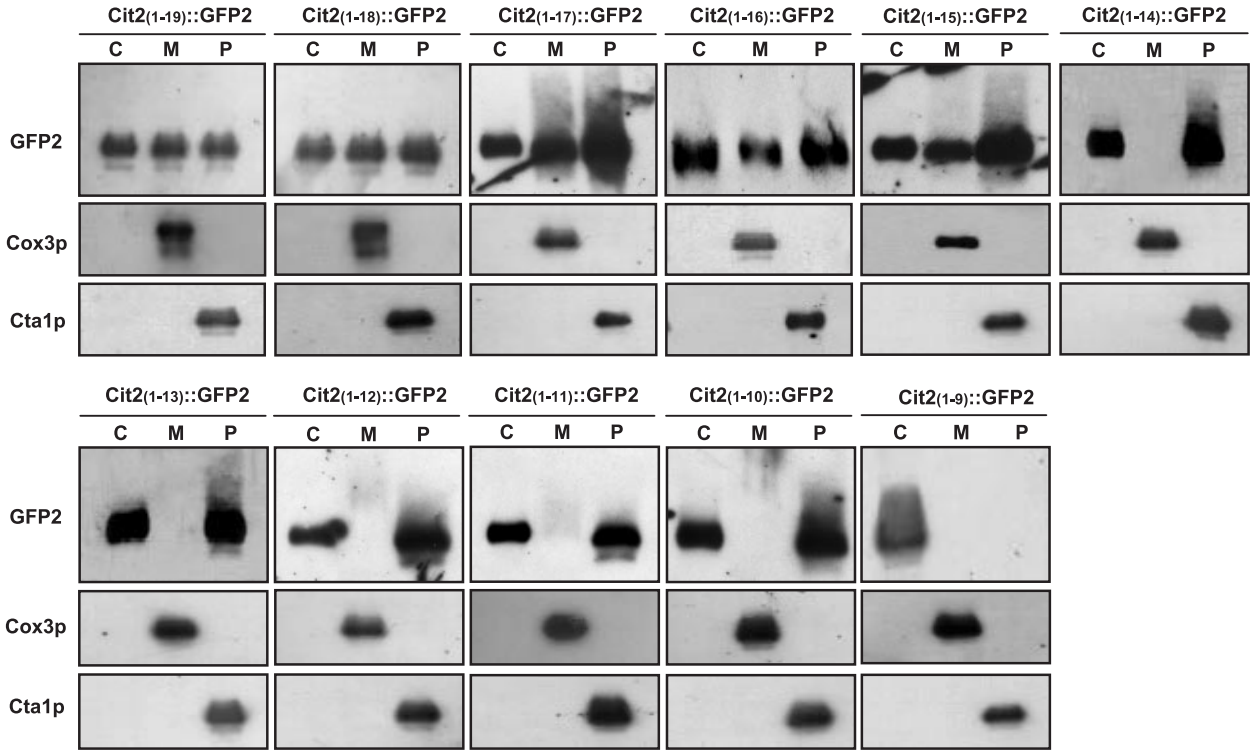

Fig. 2. **Immunoblot analysis of the subcellular distribution of the GFP2 fusion proteins carrying anteriorly fused Cit2p N-terminal segments.** Homogenized lysates of PSY37 (*CIT1 CIT2*) cells transformed with one of the plasmids carrying the chimeric genes encoding the fusion proteins of the Cit2p N-terminal segments were fractionated by ultracentrifugation to yield cytosolic (C), mitochondrial (M), and peroxisomal (P) fractions. The proteins were separated by SDS-PAGE on a 12.5% acrylamide gel. The GFP2 fusion proteins were detected with the use of rabbit anti-GFP as a primary antibody, cytochrome c oxidase with mouse monoclonal anti-Cox3p, and catalase A with rabbit anti-Cta1p.

analysis, this result also supports that the segment comprising from positions 16 to 20 of Cit2p is excluded from the cryptic N-terminal targeting signal but also completely ineffective on the function of the signal.

Contrary to the expectation based on the results of serial deletion, the transformants producing the GFP2 fusion proteins, $Cit2_{(Y15A)}$::GFP2, $Cit2_{(Y15S)}$::GFP2, $Cit2_{(Y15P)}$::GFP2, and $Cit2_{(Y15F)}$::GFP2, which contained the 20–amino acid N-terminal segments of Cit2p with single amino acid substitutions of Tyr by Phe, Pro, or Ser at position 15, gave a single positive band for all three fractions, *i.e.* the cytosolic, mitochondrial and peroxisomal fractions (Fig. 3). This result indicates that mutations causing exchange of the Tyr residue at position 15 by Phe, Pro, or Ser do not affect the import of the fusion protein into either mitochondria or peroxisomes (Fig. 4A). It can be thus suggested that although the minimum extent of the cryptic N-terminal signal is 15–amino acid long, the location of a tyrosine residue at position 15 is not essential for either the MTS or PTS function of the N-terminal targeting signal.

For each of the transformants producing $Cit2_{(Y15A)}$::GFP2, $Cit2_{(S14A)}$::GFP2, $YEpCit2_{(V12A)}$::GFP2, $Cit2_{(N11A)}$::GFP2, $Cit2_{(R10A)}$::GFP2, $Cit2_{(N9A)}$::GFP2, $Cit2_{(Y5A)}$::GFP2, $Cit2_{(P4A)}$::GFP2, and $Cit2_{(T2A)}$::GFP2 fusion proteins, respectively, a single protein band of ~27 kDa recognized by anti-GFP antibodies was detected for the cytosolic, mitochondrial, and peroxisomal fractions (Fig. 3). This result supports that each of the nine GFP2 fusion proteins with mutant versions of the 15–amino acid

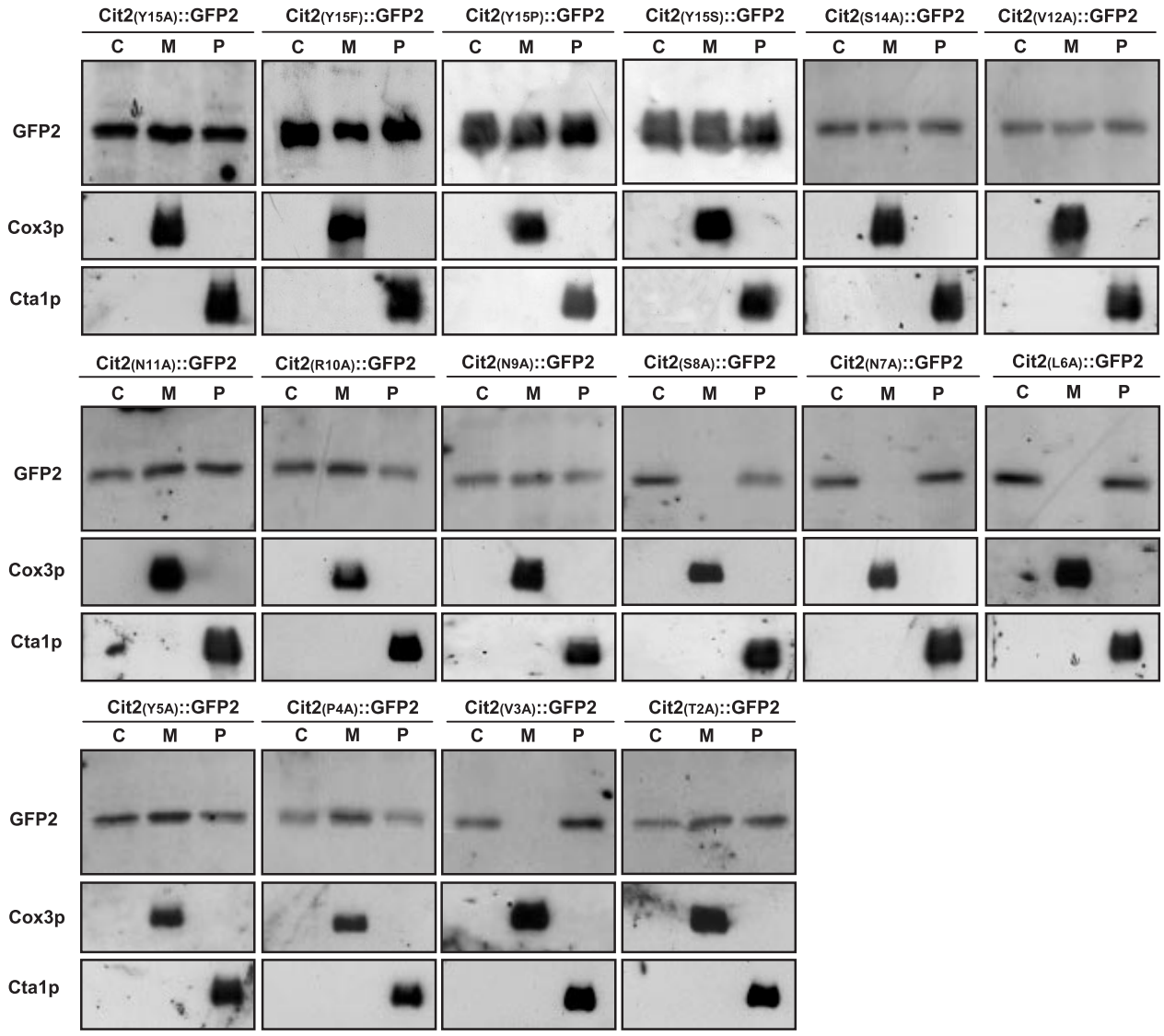

Fig. 3. **Immunoblot analysis of the subcellular distribution of the GFP2 fusion proteins carrying anteriorly fused Cit2p N-terminal segments with single amino acid substitutions.** Homogenized lysates of PSY37 (*CIT1 CIT2*) cells transformed with one of the plasmids carrying the chimeric genes encoding the fusion proteins of the Cit2p N-terminal segments with single amino acid substitutions and GFP2 were fractionated by ultracentrifugation to yield cytosolic (C), mitochondrial (M), and peroxisomal (P) fractions. The proteins were separated by SDS-PAGE on a 12.5% acrylamide gel. The GFP2 fusion proteins were detected with the use of rabbit anti-GFP as a primary antibody, cytochrome c oxidase (a marker protein for the mitochondrial fraction) with mouse monoclonal anti-Cox3p, and catalase A (a marker protein for the mitochondrial fraction) with rabbit anti-Cta1p.

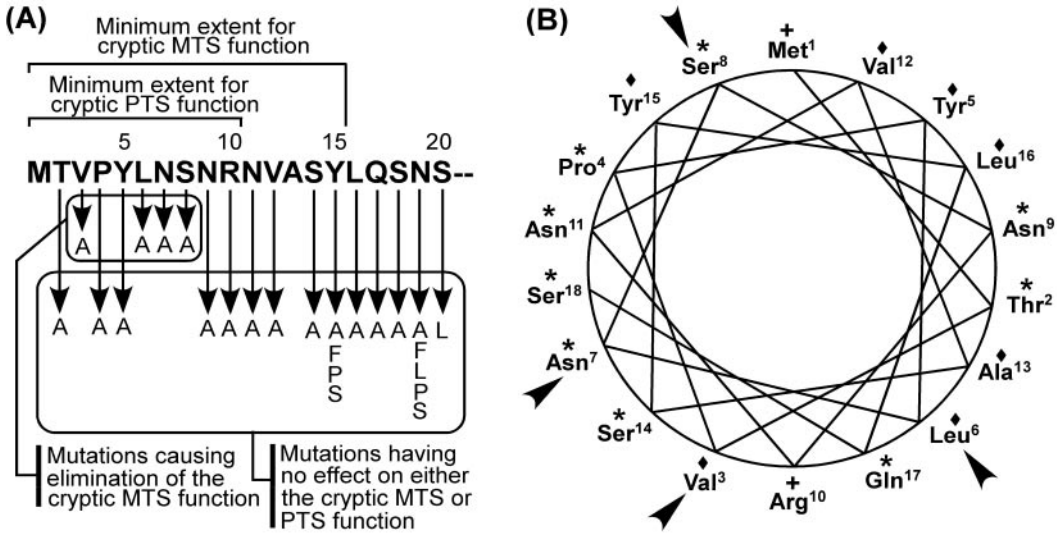

Fig. 4. **Fine structure of the cryptic ambidextrous organelle targeting signal in the N-terminal segment of Cit2p.** (A) Summarized presentation of the results of deletion and substitution analysis of the N-terminal segment of Cit2p. (B) A presumptive α-helical wheel structure that might be formed by the N-terminal segment of Cit2p. Symbols: diamonds, hydrophobic amino acid; +, basic amino acid; *, uncharged polar amino acid; arrowhead, amino acid essential for cryptic MTS function.

N-terminal segment of Cit2p can be imported into both mitochondria and peroxisomes. Thus none of the single amino acid substitutions, such as Y15A, S14A, V12A, N11A, R10A, N9A, Y5A, P4A, and T2A, seems to have any meaningful effect on either the cryptic MTS or PTS function of the N-terminal targeting signal of Cit2p (Fig. 4A).

On the contrary, in the cell lysates from the transformants of YEpCit2$_{(S8A)}$::GFP2, YEpCit2$_{(N7A)}$::GFP2, YEpCit2$_{(L6A)}$::GFP2, and YEpCit2$_{(V3A)}$::GFP2, protein bands recognized by anti-GFP antibodies appeared for both the cytosolic and peroxisomal fractions, but not for the mitochondrial fraction (Fig. 3). This result indicates that the four fusion proteins, Cit2$_{(S8A)}$::GFP2, Cit2$_{(N7A)}$::GFP2, Cit2$_{(L6A)}$::GFP2, and Cit2$_{(V3A)}$::GFP2, retained the function of PTS but lost that of MTS due to any one the single amino acid substitutions, such as S8A, N7A, L6A, and V3A. It is thus clear that each of the four amino acid residues, Ser, Asn, Leu, and Val, at positions 8, 7, 6, and 3, respectively, is essential for the cryptic and subtle MTS function of the N-terminal segment of Cit2p, but not for its PTS function (Fig. 4A).

We could not find any single substitutions of the amino acids that have any influence on the PTS function of the 20–amino acid N-terminal segment of Cit2p (Fig. 3). Therefore it seems that the introduction of any single substitution does not affect the PTS function of the N-terminal segment of Cit2p, and that substitutions of at least two amino acid residues are required to abolish the PTS function of the segment.

Functional Analysis of the N-Terminal Targeting Signal of Cit2p—In order to determine the physiological function of the N-terminal targeting signal of Cit2p, the recombinant plasmids, *i.e.* YEpCit1, YEpCit1$_{(\Delta N)}$, YEpCit1$_{(SKL)}$, YEpCit1$_{(\Delta N\text{-}SKL)}$, YEpCit2, YEpCit2$_{(\Delta N)}$, YEpCit2$_{(\Delta SKL)}$, and YEpCit2$_{(\Delta N\Delta SKL)}$, encoding Cit1p, Cit1$_{(\Delta N)}$p (Cit1p with deletion of the MTS), Cit1$_{(SKL)}$p (Cit1p with an additional C-terminal SKL sequence, PTS1), Cit1$_{(\Delta N\text{-}SKL)}$p (Cit1p with deletion of the 38–amino acid N-terminal MTS but an additional PTS1), Cit2p, Cit2$_{(\Delta N)}$p (Cit2p with deletion of the 15–amino acid N-terminal segment), Cit2$_{(\Delta SKL)}$p (Cit2p with deletion of the C-terminal SKL sequence), and Cit2$_{(\Delta N\Delta SKL)}$p protein (Cit2p with deletion of both the 15–amino acid N-terminal segment and the C-terminal SKL sequence), respectively, were constructed and introduced individually into *S. cerevisiae* MPY001 (*cit1::LEU2 cit2::ura3–508*) (*10*).

Cultural characteristics of the transformants were observed on YPD, YNB/UL (YNB with uridine and leucine), and YNB/ULG (YNB with uridine, leucine, and glutamate) plates in comparison with those of the control strains, such as wild type PSY37 (*CIT1 CIT2*), PSY38 (*cit1::LEU2 CIT2*), PSY40 (*CIT1 cit2::URA3*), and MPY001 (Fig. 5A). All the yeast strains developed normal sized colonies after 3-day cultivation on YPD plates, which indicates that neither of the two citrate synthase genes is essential for the growth on the complete medium containing glucose as a sole carbon source. As expected, the Δ*cit1* Δ*cit2* double mutant (MPY001) grew on YNB/ULG, however, it failed to grow on YNB/UL plates, which confirms that mutation of both the *CIT1* and *CIT2* genes causes auxotrophy for glutamate (*10*, *14*). The Δ*cit1* Δ*cit2* strains carrying any one of the constructs, *i.e.* YEpCit1, YEpCit1$_{(SKL)}$, YEpCit2, YEpCit2$_{(\Delta N)}$, YEpCit2$_{(\Delta SKL)}$, or YEpCit2$_{(\Delta N\Delta SKL)}$, grew well on YNB/UL plates, while that harboring either YEpCit1$_{(\Delta N)}$ or YEpCit1$_{(\Delta N\text{-}SKL)}$ did not. This result shows that glutamate auxotrophy caused by double disruption of *CIT1* and *CIT2* is restored by any one of the mutant proteins derived from Cit1p or Cit2p, i.e. Cit1$_{(SKL)}$p, Cit2$_{(\Delta N)}$p, Cit2$_{(\Delta SKL)}$p, or Cit2$_{(\Delta N\Delta SKL)}$p, except for the Cit1p variants lacking N-terminal MTS, i.e. Cit1$_{(\Delta N)}$p and Cit1$_{(\Delta N\text{-}SKL)}$p. Citrate synthase activity in the cell lysates of the transformants expressing any one of the variants derived from Cit1p or Cit2p was assayed in comparison with that of the control strains (Fig. 5B). While at least 40% of the citrate synthase activity of the wild type

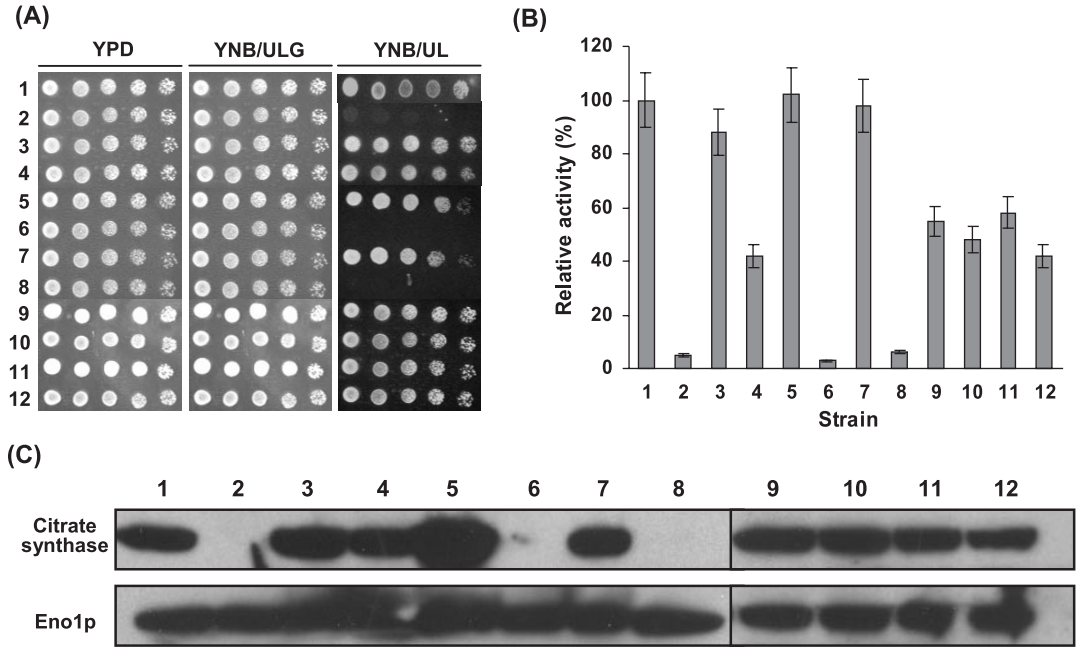

Fig. 5. **Analysis of glutamate auxotrophy and citrate synthase in *S. cerevisiae* strains.** (A) Plate assay for nutritional requirement. Cells grown overnight in liquid YPD (2% glucose) were washed and suspended in phosphate-buffered saline (PBS, pH 7.4) to the concentration of 1.0×10^8 cells ml^{-1}. After the cell suspensions had been serially diluted in 10-fold step, a 3 μl aliquot of each dilution was applied on YPD, YNB/UL (YNB with uridine and leucine), and YNB/ULG (YNB with uridine, leucine, and glutamate) plates, and the plates were incubated at 30°C for 3 days. (B) Analysis of citrate synthase activity. Homogenized lysates of *S. cerevisiae* cells grown overnight in liquid YPD were assayed for citrate synthase by the 5,5′-dithiobis-(2-nitrobenzoic acid) (DTNB) method. (C) Immunoblot analysis of citrate synthase. Proteins from the lysates of *S. cerevisiae* were separated by SDS-PAGE on a 12.5% acrylamide gel. The citrate synthase was detected with the use of rabbit anti-Cit1p as a primary antibody (*10*), and an internal reference, enolase (Eno1p), was detected with mouse anti-Eno1p. The secondary antibody was horseradish peroxidase-conjugated anti-rabbit IgG (Kirkegaard and Perry). Strains: 1, wild-type; 2, Δ*cit1*Δ*cit2*; 3, Δ*cit2*; 4, Δ*cit1*; 5, Δ*cit1*Δ*cit2*/YEpCit1; 6, Δ*cit1*Δ*cit2*/YEpCit1$_{(\Delta N)}$; 7, Δ*cit1*Δ*cit2*/YEpCit1$_{(SKL)}$; 8, Δ*cit1*Δ*cit2*/YEpCit1$_{(\Delta N\text{-}SKL)}$; 9, Δ*cit1*Δ*cit2*/YEpCit2; 10, Δ*cit1*Δ*cit2*/YEpCit2$_{(\Delta SKL)}$; 11, Δ*cit1*Δ*cit2*/YEpCit2$_{(\Delta N)}$; 12, Δ*cit1*Δ*cit2*/YEpCit2$_{(\Delta N\Delta SKL)}$.

strain was detected for the transformants harboring either YEpCit1, YEpCit1$_{(SKL)}$, YEpCit2, YEpCit2$_{(\Delta N)}$, YEpCit2$_{(\Delta SKL)}$, or YEpCit2$_{(\Delta N\Delta SKL)}$, only negligible activity was observed for the YEpCit1$_{(\Delta N)}$ and YEpCit1$_{(\Delta N\text{-}SKL)}$ transformants. In parallel, immunoblot analysis of the cell lysates from the transformants was performed by using anti-Cit1p antibodies which were previously shown to recognize not only Cit1p but also Cit2p and their derivatives (*10*, *14*). In accordance with the results of enzyme assaying, no visible signals of the citrate synthases without the N-terminal MTS, *i.e.* Cit1$_{(\Delta N)}$p and Cit1$_{(\Delta N\text{-}SKL)}$p, were detected for the YEpCit1$_{(\Delta N)}$ and YEpCit1$_{(\Delta N\text{-}SKL)}$ transformants (Fig. 5C). These results suggest that the presence of any active citrate synthase in mitochondria, peroxisomes, or cytosol suffices for abolition of the glutamate auxotrophy of the Δ*cit1* Δ*cit2* mutant by supplying citrate, which is expected to be converted into glutamate *via* α-ketoglutarate. Accordingly, the incompetence of Cit1$_{(\Delta N)}$p and Cit1$_{(\Delta N\text{-}SKL)}$p as to complementation of the glutamate auxotrophy seems to be due to the loss of stability caused by deletion of the N-terminal MTS. It has been reported that the specific activity of the cytosolic form of Cit1p, *i.e.* δLSCit1p [same as Cit1$_{(\Delta N)}$p in the present study], is only 5% of that of the wild-type mitochondrial form, which suggests that the cytosolic form of Cit1p lacking the N-terminal MTS is unstable in the cytosolic compartment (*15*). Correspondingly, it is also suggested that the peroxisomal form of Cit1p lacking the N-terminal MTS, Cit1$_{(\Delta N\text{-}SKL)}$p, is unstable even in the peroxisomal compartment. Considering the absence of any targeting signals for either mitochondria or peroxisomes in Cit2$_{(\Delta N\Delta SKL)}$p, it appears that neither the C-terminal PTS1 nor the 15–amino acid N-terminal cryptic signal of Cit2p is required for suppression of the glutamate auxotrophy.

On YPA media containing 2% acetate as a sole carbon source (regardless of whether solid or liquid), both the *CIT1* strains (PSY37 and PSY40), and the Δ*cit1* Δ*cit2* mutant (MPY001) harboring YEpCit1 or YEpCit1$_{(SKL)}$ showed normal growth after 3-day cultivation (Fig. 6A and B). On the other hand, the Δ*cit1* (PSY38) and Δ*cit1* Δ*cit2* (MPY001) mutants showed only negligible growth even after 12-day cultivation. Similarly, the transformant carrying YEpCit1$_{(\Delta N)}$, YEpCit1$_{(\Delta N\text{-}SKL)}$, YEpCit2, YEpCit2$_{(\Delta N)}$, or YEpCit2$_{(\Delta N\Delta SKL)}$ did not show any meaningful signs of growth on acetate. Considering the efficient targeting of Cit1p and Cit1$_{(SKL)}$p proteins to mitochondria in comparison with the failure of Cit1$_{(\Delta N)}$p, Cit1$_{(\Delta N\text{-}SKL)}$p, Cit2p, and Cit2$_{(\Delta N\Delta SKL)}$p as to mitochondrial targeting, it is suggested that targeting of citrate synthase to mitochondria is indispensable for growth on acetate, which is consistent with the results obtained by Vélot *et al.* (*15*). Interestingly, the YEpCit2$_{(\Delta SKL)}$ transformant grew to some extent after prolonged incubation on YPA plates (Fig. 6A). The ability of the YEpCit2$_{(\Delta SKL)}$ transformant

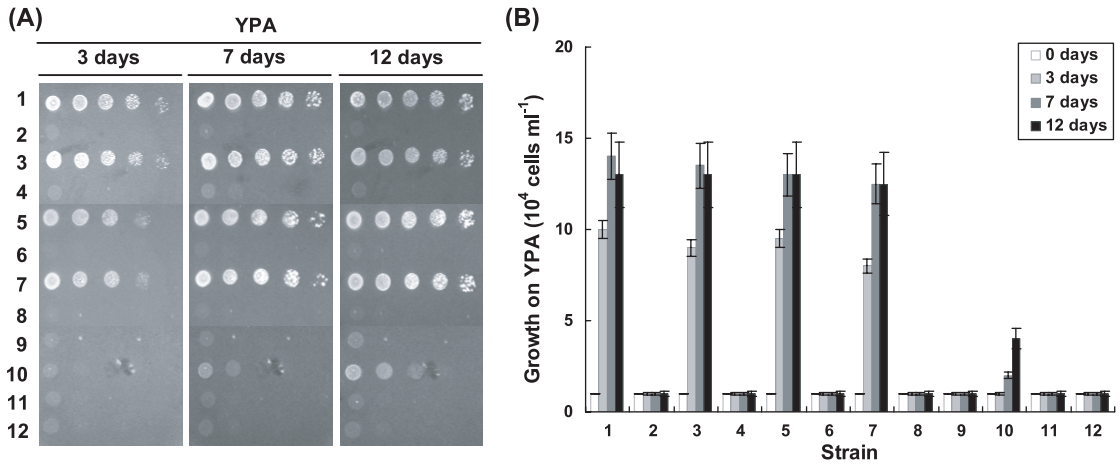

Fig. 6. **Analysis of the growth characteristics of *S. cerevisiae* strains on acetate.** (A) Cells grown overnight in liquid YPD (2% glucose) were washed and suspended in phosphate-buffered saline (PBS, pH 7.4) to the concentration of 1.0×10^8 cells ml^{-1}. After the cell suspensions had been serially diluted in 10-fold steps, a 3 μl aliquot of each dilution was applied on YPA (2% acetate) plates, and the plates were incubated at 30°C for 3–12 days. (B) For growth assaying in YPA liquid medium, aliquots of the cell suspension were inoculated into YPA liquid media at the concentration of 1.0×10^4 cells ml^{-1} and the cells were grown with shaking at 30°C. Strains: 1, wild-type; 2, Δ*cit1*Δ*cit2*; 3, Δ*cit2*; 4, Δ*cit1*; 5, Δ*cit1*Δ*cit2*/YEpCit1; 6, Δ*cit1*Δ*cit2*/YEpCit1$_{(\Delta N)}$; 7, Δ*cit1*Δ*cit2*/YEpCit1$_{(SKL)}$; 8, Δ*cit1*Δ*cit2*/YEpCit1$_{(\Delta N\text{-}SKL)}$; 9, Δ*cit1*Δ*cit2*/YEpCit2; 10, Δ*cit1*Δ*cit2*/YEpCit2$_{(\Delta SKL)}$; 11, Δ*cit1*Δ*cit2*/YEpCit2$_{(\Delta N)}$; 12, Δ*cit1*Δ*cit2*/YEpCit2$_{(\Delta N\Delta SKL)}$.

to grow on acetate was also confirmed by growth assaying in YPA liquid medium, although it showed a much longer lag phase and a slower growth rate than the *CIT1* strains and the multi-copy transformant carrying YEpCit1 or YEpCit1$_{(SKL)}$ (Fig. 6B). The slow growth of the YEpCit2$_{(\Delta SKL)}$ transformant on acetate seems to be a reflection of the possibility that a minor portion of Cit2$_{(\Delta SKL)}$p is targeted to mitochondria through the action of its 15–amino acid N-terminal segment.

DISCUSSION

We previously reported that the 15–amino acid N-terminal segment of Cit2p is cleaved during its import into peroxisomes despite the presence of a C-terminal PTS1 (*8*), and that an ambidextrous signal for both peroxisomes and mitochondria is included within the 20–amino acid N-terminal segment of Cit2p (*10*). In an attempt to define the minimum extents of the cryptic signals for mitochondrial and peroxisomal targeting, we performed serial deletion analysis, and found that the minimum extent of the cryptic mitochondrial targeting signal of Cit2p consists of the 15–amino acid N-terminal segment, while that of the cryptic peroxisomal targeting signal consists of the 10–amino acid N-terminal segment.

Many precursor proteins destined for mitochondria contain N-terminal presequences or MTSs with 12–80 amino acid residues that are rich in positively charged ones and have the potential to form an amphiphilic α-helix (*16–18*). The presequence is recognized by receptors embedded in the mitochondrial outer membrane (TOM) and inner membrane (TIM). The cytosolic domains of three import receptors, Tom20, Tom22, and Tom70, have been shown to interact with the MTSs contained in mitochondrial preproteins (*19*, *20*). The Tim23·17 complex then mediates the translocation of an MTS across the inner membrane in a Δψ-dependent manner (*21*, *22*), and finally Tim44, and mt-Hsp70 and Mge1 receive the presequence on the inner side of the inner membrane to mediate the translocation of the precursors across both membranes in an ATP-dependent manner (*23*, *24*). Although the mechanism of recognition of MTS by the translocases TOM and TIM in the process of mitochondrial protein import has not been fully characterized yet, the molecular mechanism for the interaction between the presequence of rat aldehyde dehydrogenase (ALDH) and Tom20 has been well characterized (*25–27*). The positive charges of MTS are essential for the mitochondrial import ability, however, presequence binding to Tom20 is mediated mainly by a hydrophobic rather than an ionic interaction (*25*). A common motif required for the interaction between an MTS and Tom20 has been found to be ΦχχΦΦ, where Φ is a hydrophobic/aromatic residue and χ is any amino acid residue (*26*).

The N-terminal segment of Cit2p does not seem to have either the ΦχχΦΦ motif for binding to Tom20 or high potential for authentic α-helix formation, which reflects the poor mitochondrial targeting efficiency of Cit2p. A presumptive helical wheel of the first 18–amino acid residues, however, shows some similarity to that of conventional MTSs (Fig. 4B). In the presumptive helical wheel structure, the hydrophobic and hydrophilic faces are separated from each other, and hydroxylated amino acid residues such as Ser and Tyr appear frequently. However, distinctively from the authentic MTSs, the presequence of Cit2p contains only one positively charged amino acid, Arg. The N-terminal segment of Cit2p with 10–14 amino acids did not guide the reporter protein to mitochondria although it retained weak PTS activity. This result supports the prediction that no N-terminal segment of Cit2p containing less than the first 15 amino acids can form even a fragile MTS, but still can function as a weak PTS. The effects of amino acid deletion observed in the present study may not reflect interactions with any single receptor protein in mitochondria, but instead may represent the sum of the

effects on some of the above mitochondrial components/factors during protein import. Thus more sophisticated experiments involving mutants with defects in the Tom and/or Tim proteins are required to determine the exact structure of the N-terminal presequence of Cit2p as well as the mitochondrial import pathway for Cit2p.

Quite similarly to the case of MTSs, the N-terminal amino acid residues at positions 1–40, which are relatively enriched in positively charged ones, are required for translocation of Pex3p, an integral membrane peroxin, to peroxisomes in mammals and yeast (*28–30*). Positively charged amino acids are also functionally important in the PTS of peroxisomal membrane proteins, *i.e.* mPTS. For instance, the loop region between the fourth transmembrane segment (TM4) and TM5 of a peroxisomal membrane protein, PMP47, of yeast *Candida boisini*, which spans the membrane six times, is enriched in positively charged amino acids and is functional as a PTS when fused to cytosolic proteins (*31*). Human PMP34 protein, an ortholog of PMP47, is also directly imported into peroxisomes after its synthesis on cytoplasmic polysomes by a potential mTPS, *i.e.* the loop region between TM4 and TM5. When the basic amino acids of the loop region are replaced by a small nonpolar amino acid, Ala, the protein fails as to targeting to peroxisomes (*32*).

In the present study, we found that at least the first 10 N-terminal amino acids are involved in the atypical and cryptic PTS function of the N-terminal segment of Cit2p. However, the N-terminal segment is quite distinct from any of the authentic N-terminal or internal PTSs, because it contains neither the RXKKK nor the RL-XXXXX-HL motif. It is thus expected that the N-terminal segment of Cit2p can function as only a weak peroxisomal targeting signal. In addition, the absence of any authentic PTS motifs, such as the PTS2 motif, in the N-terminal segment of Cit2p raises the question of the route of the peroxisomal import mediated by the segment. In the previous report, we showed that neither the *pex5* nor the *pex7* mutation affects the targeting behavior of the $Cit2_{(1–20)}$::GFP2 protein containing the N-terminal segment of Cit2p and, accordingly, that the mitochondrial and peroxisomal targeting processes mediated by this segment do not require either Pex5p or Pex7p (*10*).

To define the amino acid residues essential to the function of the cryptic N-terminal signal of Cit2p for mitochondrial and/or peroxisomal targeting, we introduced single amino acid substitutions, and analyzed the effects of the substitutions on the targeting activity of the segment. Unexpectedly, Ala substitution for the 10th Arg did not abolish either the MTS or PTS activity of the N-terminal segment, which implies that the internal positive charge of the presequence is not indispensable. On the contrary, each of the substitutions, S8A, N7A, L6A, and V3A, impaired the MTS function without weakening the PTS function. It is thus suggested that not only the 8th Ser and the 7th Asn in the hydrophilic face but the 6th Leu and 3rd Val in the hydrophobic face play a crucial role in maintaining the weak MTS activity. Accordingly, it has been suggested that small amino acids, such as Ala, are likely to disturb the formation of a weak α-helical wheel (*33*). Quite differently from the case of the MTS function, we could not find any single substitution mutation impairing the peroxisomal targeting capacity. This result indicates that none of the individual amino acid residues are crucial for the PTS function of the N-terminal segment of Cit2p and that substitutions of at least two amino acids would be required to abolish its PTS function.

All the active variants derived from Cit1p and Cit2p [$Cit1_{(SKL)}$p, $Cit2_{(\Delta N)}$p, $Cit2_{(\Delta SKL)}$p, and $Cit2_{(\Delta N\Delta SKL)}$p], except for the unstable ones from Cit1p lacking the N-terminal MTS [$Cit1_{(\Delta N)}$p and $Cit1_{(\Delta N\text{-}SKL)}$p], restored the glutamate auxotrophy caused by the double Δ*cit1* Δ*cit2* mutation. This suggests that the presence of either citrate synthase in any of the three compartments of a cell, i.e. mitochondria, peroxisomes, or cytosol, is sufficient to abolish the glutamate auxotrophy. Accordingly, it appears that neither the C-terminal PTS1 nor the 15–amino acid N-terminal cryptic signal of Cit2p is required for suppression of the auxotrophy. The incompetence as to acetate utilization caused by the Δ*cit1* mutation was fully restored by either Cit1p or $Cit1_{(SKL)}$p carrying an authentic MTS, but not by any other variants lacking an MTS [$Cit1_{(\Delta N)}$p, $Cit1_{(\Delta N\text{-}SKL)}$p, Cit2p, or $Cit2_{(\Delta N\Delta SKL)}$p]. This indicates that localization of citrate synthase in the specific cellular compartment, *i.e.* mitochondria, is essential for utilization of acetate as a sole carbon and energy source. In addition, this result is in good agreement with the previous report that Cit2p is able to restore the growth of a yeast strain lacking Cit1p on acetate when mislocalized to mitochondria by N-terminally fused MTS, while the cytosolically localized form of either Cit1p or Cit2p is not (*15*). The reason why the localization of citrate synthase to mitochondria is indispensable for restoration of growth on acetate can be explained by the idea of a TCA multienzyme complex, which requires the structural contribution of the mitochondrial citrate synthase, Cit1p, for TCA cycle functions (*34–36*). In addition, the peroxisomal citrate synthase, Cit2p, when mislocalized to mitochondria, seems to be able to mimic its mitochondrial isoform, Cit1p, in the TCA multienzyme complex (*15*). It was found in the present study that $Cit2_{(\Delta SKL)}$p can restore the growth of the Δ*cit1* Δ*cit2* mutant (or Δ*cit1* mutant) on acetate, although much less efficiently than either Cit1p or $Cit1_{(SKL)}$p carrying an authentic MTS, while either Cit2p or $Cit2_{(\Delta N\Delta SKL)}$p can not. This result is in good accordance with the previous finding that a minor portion of $Cit2_{(\Delta SKL)}$p is targeted to mitochondria (*37*). Considering the presence of both the 15–amino acid N-terminal segment and the authentic C-terminal peroxisomal targeting signal, PTS1, in Cit2p and its failure to restore the growth of the Δ*cit1* Δ*cit2* mutant on acetate, it is suggested that elimination of the C-terminal SKL (PTS1) unmasks the cryptic function of the N-terminal segment of Cit2p as an ambidextrous targeting signal for both organelles.

A few proteins carrying PTS1 have been reported to contain extra PTSs. Cta1p of *S. cerevisiae* contains two independent signals, a C-terminal SSNSKF motif and the N-terminal third segment of the protein, each of which is sufficient for targeting of a protein to peroxisomes (*38*). Per1p of *H. polymorpha*, which plays an essential role in peroxisome proliferation, similarly contains both a PTS1 and an N-terminal PTS (PTS2) (*39*). However, there have been no other reports on such a protein containing an additional N-terminal ambidextrous organelle targeting signal. Instead, an informative implication can be derived

from the results of mutational analysis of the N-terminal presequence (PTS2) of the rat peroxisomal 3-ketoacyl-CoA thiolase precursor, which showed that substitution of the Glu residue at position –11 (11-residue upstream from the cleavage site of the precursor protein) with an amino acid other than Asp converts the PTS2 into an ambidextrous signal for both peroxisomal and mitochondrial targeting (*40*). For now, we cannot explain exactly how the Cit2p destined for peroxisomes came to have the N-terminal cryptic ambidextrous targeting signal in addition to the C-terminal PTS1. It has been suggested from the aspect of molecular evolution that one of the two citrate synthase genes of *S. cerevisiae* (*CIT1* and *CIT2*) arose through gene duplication of the other, followed by sequence divergence to create an MTS or a PTS1 (*5*).

This work was supported by Non-Directed Research Funds (Project No. 1998-001-D00762), Korea Research Foundation, 1998. We wish to thank Dr. Hee-Moon Park, Chungnam National University, Korea, for the mouse anti-Eno1p antibody.

REFERENCES

1. Slupphaug, G., Markussen, F.H., Olsen, L.C., Aasland, R., Aarsaether, N., Bakke, O., Krokan, H.E., and Helland, D.E. (1993) Nuclear and mitochondrial forms of human uracil-DNA glycosylase are encoded by the same gene. *Nucleic Acids Res.* **21**, 2579–2584
2. Oda, T., Funai, T., and Ichiyama, A. (1990) Generation from a single gene of two mRNAs that encode the mitochondrial and peroxisomal serine:pyruvate aminotransferase of rat liver. *J. Biol. Chem.* **265**, 7513–7519
3. Szewczyk, E., Andrianopoulos, A., Davis, M.A., and Hynes, M.J. (2001) A single gene produces mitochondrial, cytoplasmic, and peroxisomal NADP-dependent isocitrate dehydrogenase in *Aspergillus nidulans*. *J. Biol. Chem.* **276**, 37722–37729
4. Suissa, M., Suda, K., and Schatz, G. (1984) Isolation of the nuclear yeast genes for citrate synthase and fifteen other mitochondrial proteins by a new screening method. *EMBO J.* **3**, 1773–1781
5. Rosenkrantz, M., Alam, T., Kim, K.S., Clark, B.J., Srere, P.A., and Guarente, L.P. (1986) Mitochondrial and nonmitochondrial citrate synthases in *Saccharomyces cerevisiae* are encoded by distinct homologous genes. *Mol. Cell. Biol.* **6**, 4509–4515
6. Jia, Y.K., Becam, A.M., and Herbert, C.J. (1997) The *CIT3* gene of *Saccharomyces cerevisiae* encodes a second mitochondrial isoform of citrate synthase. *Mol. Microbiol.* **24**, 53–59
7. Lewin, A.S., Hines, V., and Small, G.M. (1990) Citrate synthase encoded by the *CIT2* gene of *Saccharomyces cerevisiae* is peroxisomal. *Mol. Cell. Biol.* **10**, 1399–1405
8. Cho, N.S., Kim, K.S., and Maeng, P.J. (1991) Purification and characterization of nonmitochondrial citrate synthase from *Saccharomyces cerevisiae*. *Kor. J. Microbiol.* **29**, 230–237
9. Lee, H.S., Choi, W.S., Lee, J.S., and Maeng, P.J. (1994) Organelle targeting of citrate synthases in *Saccharomyces cerevisiae*. *Kor. J. Microbiol.* **32**, 558–564
10. Lee, J.G., Cho, S.P., Lee, H.S., Lee, C.H., Bae, K.S., and Maeng, P.J. (2000) Identification of a cryptic N-terminal signal in *Saccharomyces cerevisiae* peroxisomal citrate synthase that functions in both peroxisomal and mitochondrial targeting. *J. Biochem.* **128**, 1059–1072
11. Ito, H., Fukuda, Y., Murata, K., and Kimura, A. (1983) Transformation of intact yeast cells treated with alkali cations. *J. Bacteriol.* **153**, 163–168
12. Sambrook, J. and Russell, D.W. (2001) *Molecular Cloning: A Laboratory Manual*. 3 ed. (Irwin, N. and Janssen, K.A., eds.) 3 vols., Cold Spring Harbor Laboratory Press, Cold Spring Harbor, New York
13. Srere, P.A. (1969) Citrate synthase. *Methods Enzymol.* **13**, 3–26
14. Kim, K.S., Rosenkrantz, M.S., and Guarente, L. (1986) *Saccharomyces cerevisiae* contains two functional citrate synthase genes. *Mol. Cell. Biol.* **6**, 1936–1942
15. Velot, C., Lebreton, S., Morgunov, I., Usher, K.C., and Srere, P.A. (1999) Metabolic effects of mislocalized mitochondrial and peroxisomal citrate synthases in yeast *Saccharomyces cerevisiae*. *Biochemistry* **38**, 16195–16204
16. Roise, D. and Schatz, G. (1988) Mitochondrial presequences. *J. Biol. Chem.* **263**, 4509–4511
17. Roise, D., Theiler, F., Horvath, S.J., Tomich, J.M., Richards, J.H., Allison, D.S., and Schatz, G. (1988) Amphiphilicity is essential for mitochondrial presequence function. *EMBO J.* **7**, 649–653
18. Roise, D., Horvath, S.J., Tomich, J.M., Richards, J.H., and Schatz, G. (1986) A chemically synthesized pre-sequence of an imported mitochondrial protein can form an amphiphilic helix and perturb natural and artificial phospholipid bilayers. *EMBO J.* **5**, 1327–1334
19. Brix, J., Dietmeier, K., and Pfanner, N. (1997) Differential recognition of preproteins by the purified cytosolic domains of the mitochondrial import receptors Tom20, Tom22, and Tom70. *J. Biol. Chem.* **272**, 20730–20735
20. Brix, J., Rudiger, S., Bukau, B., Schneider-Mergener, J., and Pfanner, N. (1999) Distribution of binding sequences for the mitochondrial import receptors Tom20, Tom22, and Tom70 in a presequence-carrying preprotein and a non-cleavable preprotein. *J. Biol. Chem.* **274**, 16522–16530
21. Berthold, J., Bauer, M.F., Schneider, H.C., Klaus, C., Dietmeier, K., Neupert, W., and Brunner, M. (1995) The MIM complex mediates preprotein translocation across the mitochondrial inner membrane and couples it to the mt-Hsp70/ATP driving system. *Cell* **81**, 1085–1093
22. Horst, M., Hilfiker-Rothenfluh, S., Oppliger, W., and Schatz, G. (1995) Dynamic interaction of the protein translocation systems in the inner and outer membranes of yeast mitochondria. *EMBO J.* **14**, 2293–2297
23. Kronidou, N.G., Oppliger, W., Bolliger, L., Hannavy, K., Glick, B.S., Schatz, G., and Horst, M. (1994) Dynamic interaction between Isp45 and mitochondrial hsp70 in the protein import system of the yeast mitochondrial inner membrane. *Proc. Natl. Acad. Sci. USA* **91**, 12818–12822
24. Schneider, H.C., Berthold, J., Bauer, M.F., Dietmeier, K., Guiard, B., Brunner, M., and Neupert, W. (1994) Mitochondrial Hsp70/MIM44 complex facilitates protein import. *Nature* **371**, 768–774
25. Abe, Y., Shodai, T., Muto, T., Mihara, K., Torii, H., Nishikawa, S., Endo, T., and Kohda, D. (2000) Structural basis of presequence recognition by the mitochondrial protein import receptor Tom20. *Cell* **100**, 551–560
26. Muto, T., Obita, T., Abe, Y., Shodai, T., Endo, T., and Kohda, D. (2001) NMR identification of the Tom20 binding segment in mitochondrial presequences. *J. Mol. Biol.* **306**, 137–143
27. Obita, T., Muto, T., Endo, T., and Kohda, D. (2003) Peptide library approach with a disulfide tether to refine the Tom20 recognition motif in mitochondrial presequences. *J. Mol. Biol.* **328**, 495–504
28. Kammerer, S., Holzinger, A., Welsch, U., and Roscher, A.A. (1998) Cloning and characterization of the gene encoding the human peroxisomal assembly protein Pex3p. *FEBS Lett.* **429**, 53–60
29. Ghaedi, K., Tamura, S., Okumoto, K., Matsuzono, Y., and Fujiki, Y. (2000) The peroxin pex3p initiates membrane assembly in peroxisome biogenesis. *Mol. Biol. Cell* **11**, 2085–2102

30. Baerends, R.J., Faber, K.N., Kram, A.M., Kiel, J.A., van der Klei, I.J., and Veenhuis, M. (2000) A stretch of positively charged amino acids at the N terminus of *Hansenula polymorpha* Pex3p is involved in incorporation of the protein into the peroxisomal membrane. *J. Biol. Chem.* **275**, 9986–9995
31. Dyer, J.M., McNew, J.A., and Goodman, J.M. (1996) The sorting sequence of the peroxisomal integral membrane protein PMP47 is contained within a short hydrophilic loop. *J. Cell Biol.* **133**, 269–280
32. Honsho, M. and Fujiki, Y. (2001) Topogenesis of peroxisomal membrane protein requires a short, positively charged intervening-loop sequence and flanking hydrophobic segments. study using human membrane protein PMP34. *J. Biol. Chem.* **276**, 9375–9382.
33. Osumi, T., Tsukamoto, T., and Hata, S. (1992) Signal peptide for peroxisomal targeting: replacement of an essential histidine residue by certain amino acids converts the amino-terminal presequence of peroxisomal 3-ketoacyl-CoA thiolase to a mitochondrial signal peptide. *Biochem. Biophys. Res. Commun.* **186**, 811–818
34. Kispal, G., Evans, C.T., Malloy, C., and Srere, P.A. (1989) Metabolic studies on citrate synthase mutants of yeast. A change in phenotype following transformation with an inactive enzyme. *J. Biol. Chem.* **264**, 11204–11210
35. Morgunov, I. and Srere, P.A. (1998) Interaction between citrate synthase and malate dehydrogenase. Substrate channeling of oxaloacetate. *J. Biol. Chem.* **273**, 29540–29544.
36. Velot, C., Mixon, M.B., Teige, M., and Srere, P.A. (1997) Model of a quinary structure between Krebs TCA cycle enzymes: a model for the metabolon. *Biochemistry* **36**, 14271–14276.
37. Singh, K.K., Small, G.M., and Lewin, A.S. (1992) Alternative topogenic signals in peroxisomal citrate synthase of *Saccharomyces cerevisiae*. *Mol. Cell. Biol.* **12**, 5593–5599
38. Kragler, F., Langeder, A., Raupachova, J., Binder, M., and Hartig, A. (1993) Two independent peroxisomal targeting signals in catalase A of *Saccharomyces cerevisiae*. *J. Cell Biol.* **120**, 665–673
39. Waterham, H.R., Titorenko, V.I., Haima, P., Cregg, J.M., Harder, W., and Veenhuis, M. (1994) The *Hansenula polymorpha PER1* gene is essential for peroxisome biogenesis and encodes a peroxisomal matrix protein with both carboxy- and amino-terminal targeting signals. *J. Cell Biol.* **127**, 737–749
40. Tsukamoto, T., Hata, S., Yokota, S., Miura, S., Fujiki, Y., Hijikata, M., Miyazawa, S., Hashimoto, T., and Osumi, T. (1994) Characterization of the signal peptide at the amino terminus of the rat peroxisomal 3-ketoacyl-CoA thiolase precursor. *J. Biol. Chem.* **269**, 6001–6010